Performance Investigation of the Lifetime of Solar Cell Using Surface Photovoltage (SPV) Method and Efficiency Measurement

Nusrat Chowdhury* iD , Chowdhury Akram Hossain** iD , Michela Longo*** iD , Wahiba Yaïci**** iD

* Department of Electrical and Electronic Engineering, Daffodil International University, Dhaka 1207, Bangladesh
** Department of Electrical and Electronic Engineering, American International University-Bangladesh, Dhaka, Bangladesh
*** Department of Energy, Politecnico di Milano, Piazza Leonardo da Vinci 32, 20133 Milan, Italy
**** CanmetENERGY Research Centre, Natural Resources Canada, 1 Haanel Drive, Ottawa (Ontario), K1A 1M1 Canada

(nusrat.eee@diu.edu.bd, chowdhury.akram@aiub.edu, michela.longo@polimi.it, wahiba.yaici@canada.ca)

‡ Michela Longo; Corresponding Author, Department of Energy, Politecnico di Milano, Via La Masa, 34, 20156, Milan (MI), Italy, Email: michela.longo@polimi.it

Abstract- In this paper, the optical characterisation of mono crystalline fabricated solar cells has been investigated focusing on the minority carrier flow using surface photovoltage (SPV) technique and the efficiency of the solar cells has been evaluated by means of the sun simulator analysis.

A computer-controlled incidence measurement system was conceived for SPV evaluations based on a mini mono-chromator, which was driven by a stepper motor to various wavelengths in the spectral range of 400–1200 nm. SPV is typically quantified by means of Standard Research 510 lock-in amplifiers. A LabVIEW platform is employed for system control and data acquisition. Every step of the measurement has been described in detail throughout the completely experimental procedure. Once computing the testing data acquired from monocrystalline silicon solar cell measurement, the length (L) of the minority carrier diffusion and lifetime (τ) were evaluated and results derived were 92 µm and nearly 3.135 µs, respectively. From the experimental data we have successfully found the efficiency as 16.05% using the Sun Simulator K3000 LAB55. The results from the experimental data has promising application to assess the quality of the solar cells that are being used.

1. Introduction

The use of solar energy has grown exponentially in the last couple of decades due to its superior photoelectric conversion efficiency and durable steadiness [1,2]. Scholars are currently engaged in undertaking research studies on several types of solar cells in order to extract and appropriate the energy effectively [3,4]. Si-crystalline (mono or poly) panels are the most integrated photovoltaic technology and have dominated the PV industry for decades. Mono crystalline cell has clear orientation to the lattice, and good photoelectric conversion effectiveness appeals considerable interest. Nevertheless, the photovoltaic industry's fabrication cost is still a recent problem. Interestingly, several studies have determined that enhancing the efficiency of the solar cell conversion is a means to reduce fabrication costs [1,5]. Furthermore, improving a monocrystalline silicon solar cell with a high conversion efficiency entails lowering optical, bulk recombination, and surface losses. The large refractive index amounts present in crystalline silicon gives it a poor absorption capacity for the incident light. An estimated 30–40% of incident light is wasted due to the reflection at the leading side of the cell [6].

Among major factors that determine solar cell effectiveness is the minority carrier diffusion length. Apart from grain boundaries, diverse defects sometimes have a fundamental part in minority carrier diffusion length. Hence experimental evaluation of minority carrier lifetimes or diffusion lengths are particularly useful for material characterisation, process control and system optimisation [7,8]. Surface photovoltage (SPV) is a commonly applied method for measuring diffusion lengths in both monocrystalline and multicrystalline Si wafers. This

technique is a standard contact-free procedure for semiconductor characterisation, which depends on evaluating illumination-induced variations in the surface voltage. It has been used during the past several years as a widespread resource of surface and bulk material on numerous semiconductors and semiconductor interfaces, based on the ground breaking research of Brattain and Bardeen in the early 1950s [9].

During the cell fabrication process there are two processes of characterisation of textured surface of Si wafer. One is Surface Reflection and Response (SRR) and another is Scanning Electron Microscope (SEM). Other characterisation tests are carried out after completing the fabrication of a solar cell. These tests indicate the efficiency of a solar cell. The major characterisation equipment is Light Current Voltage (LIV) tester or sun simulator with which it was possible to assess the performance of the cell and mainly to compute the efficiency of the solar cell. Another is the SPV method, which is founded on evaluating illumination-induced variations in the surface voltage. There is also the four-point probe for measuring sheet and bulk resistance of the cell [10–13].

Solar cells are characterised by their capability to convert sunlight into electricity. To achieve high efficiency, solar cells must have adequate surface passivation and high minority carrier lifetime. It is well known that the surface recombination must be reduced to realise the maximum possible efficiency of crystalline Si solar cells. For p-type doped Si wafers, a simple, yet accurate method based on surface photovoltage was developed. This SPV minority-carrier lifetime measurement system has been designed to characterize up to 6-inch diameter Si wafers. Surface photovoltage generated by incident light is measured through a lock-in amplifier to obtain detection capacity over an very large (μV to V) scale. A LabVIEW-based computer data acquisition system is employed to obtain SPV against wavelength. A linear regression analysis of the graphed data creates the wafer minority carrier lifetime. For short wavelength ranges, this method also gives qualitative information on surface passivation.

Traditional solar cell evaluation methodologies such as illuminated current-voltage (I eV, J-V) and Suns-VOC produce a single global quantity for a solar cell's performance factors. These include the conversion efficiency (η), short-circuit current density (J_{SC}), open-circuit voltage (V_{OC}), fill factor (FF), dark saturation current density (J_0), and series resistance (R_S). Nevertheless, solar cells are bulky area systems that usually indicate considerable variations in these factors on the surface of the whole system [9,14,15]. It is well known that three major parameters, namely the open circuit voltage (V_{OC}), short circuit current density (J_{SC}), and fill factor (FF), significantly affect the power conversion effectiveness of solar cells [16]. The J_{SC} can be strengthened by the V_{OC} development of new narrow-gap materials or innovative techniques for light harvesting. The V_{OC} has a closed correlation to the recombination of non-radiative excitons, which may interface within layers or at the surface in the bulk. Moreover, implementing materials with greater band spaces can likewise enhance the V_{OC}. However, a compromise between V_{OC} and J_{SC} can be established

simultaneously. Conversely, the FF can reflect the properties of maximum power output when the solar cell has optimum load plus produces a high power conversion efficiency [16].

The SPV approach is much affordable and more accurate compared to other contact-free techniques for instance EBIC (Electron Beam Induced Current) and μ-PCD (Microwave Photoconductive Decay) [17]. The SPV produced when some of the minority carriers, which deviate nearby in the bulk attain the surface. The diffusion length is the statistical distance that carriers travel in the bulk before recombining. As a result, once they reach the surface, a few of the minority carriers reunite. In steady-state condition, the production and recombination rates are completely in equilibrium. According to Goodman hypothesis, by the measurement of SPV against wavelength, the minority carrier diffusion length can be defined [17]. Moreover, many researchers have investigated the relation between the doping concentration and minority carrier life time and they tried to find the effect of the doping concentration and wafer thickness on minority carrier life time of fabricated P-type doped solar cell [18–23].

In our work, the application of SPV to find the parameters has been implemented which contributes as a new approach to test the parameters of the cell. Hence, the present investigation is a novel research proposal and a certain contribution to knowledge.

Therefore, taking into consideration the concerns and challenges in the context of the lifetime and performance of solar cell described above, this work aims to analyse the optical characterisation of mono crystalline solar cell by surface photovoltage measurement for fabricated solar cell by evaluating minority carrier diffusion length and life time, and also to perform sun simulator testing in order to assess the performance of the cell, mainly by calculating its efficiency. To accomplish these objectives, for p-type doped Si wafers, a simple yet accurate method based on surface photovoltage was developed. In this paper two types of optical characterisations have been conducted: SPV and efficiency. A description of an experimental setup for measuring these two characterisations will feature in the first part of this paper, followed by a discussion of results of the sampled cell.

This study showed that the SPV method that has been developed for silicon solar cells may prove useful to characterising and optimising new solar cells that will be more efficient.

2. Materials and Methods

This section gives a thorough description of surface photovoltage method, estimation of minority carrier diffusion length and lifetime, and measurement of the solar cell efficiency. For the purpose of the experiment, we have tested the Cz-Si substrate of resistivity 1–3 Ω.cm, <100> orientation, and thickness was around 200 ± 20 micron, based 156 cm^2 (125 mm × 125 mm pseudo-square as cut wafer) monocrystalline silicon solar cell from IIT, India. The cell used is a p-type doped monocrystalline Si-solar cell. For

baseline depositing SiNx (silicon nitride) coating, the front contact is Ag and back contact is Al.

2.1 Surface photovoltage method

The surface photovoltage (SPV) method is a standard procedure for semiconductor characterisation on testing illumination-induced variations in the surface voltage.

If light comes on to the p-n-junction, the photons generate electron-hole sets that are disjointed by the space charge. As a result, the majority of carriers in p-type silicon are holes, the charge in the depletion region is negative, and the electric field in the depletion region pulls electrons to the surface, resulting in surface photovoltage. In the p-n-junction and the p-type area, photons are absorbed.

For electrons of diffusion length L to circulate across the n-layer, the n-layer must be suitably thin, i.e., $L \gg t$, where t is the thickness of n-layer [24–26].

When a standard 300μm thick silicon wafer is illuminated by intense sunlight of irradiance 1000 mW/cm^2, electrons and holes are produced at a rate of 9×10^{18} cm^{-3}s^{-1} [27-28]. Minority carriers that drift around in the bulk either ultimately reunite with majority carriers, otherwise they attain the surface, where they generate a surface photovoltage. The lengthier wavelength will diffuse further profoundly through the silicon, while the minority carriers produced will probably recombine prior they attain the surface. The light with lengthier wavelength is likely to generate a minor SPV signal than that with short wavelength [29]. Figure 1 shows the response of SPV signal on penetration of incident light and wave length.
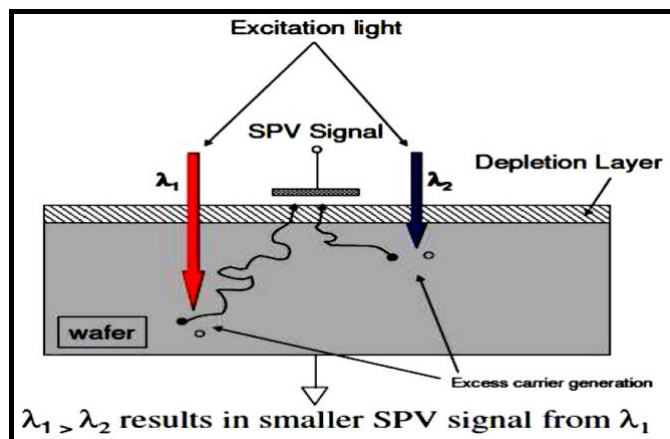
Fig. 1. SPV signal variations as a function of penetration of incident light and wavelength.

It is possible to define the diffusion length by comparing the SPV signals produced by the two diverse wavelengths. Fig. 2 shows the SPV measurement system.

The SPV method utilises the variation of the electrochemical potential in the space-charge area of a semiconductor throughout surplus carrier production attributable to irradiance of the sample with light of appropriate wavelength and concentration [29,30]. In 1961, Goodman showed that, under certain assumptions, by representing SPV measurements against wavelength, the diffusion length of the minority carrier is ascertainable. Hence, the principal aim of the SPV method is to determine the diffusion length of minority carriers within the necessary light absorption area within solar cells and wafers with dc conditions [10].

Fig. 2. SPV measurement system.

2.2 Evaluation of minority carrier diffusion length and lifetime

The minority carrier diffusion length, L, is a key parameter in determining the material's quality and transport properties. When a group of minority carriers moving nearby in the bulk reach the surface, the SPV is formed. The diffusion length is the statistical distance that carriers travel within the bulk before recombining. Due to a few of the minority carriers recombining before attaining the surface, high recombination losses mean that the smaller the diffusion length, the shorter the SPV signal.

Analysis of the potential of a light-exposed semiconductor surface is required for SPV measurements. Depletion zones are common on semiconductor surfaces, where the integrated electric field induced by defects or junction formation transports all free charge carriers. A lower carrier density indicates that most of the carriers' electronic energy bands are bent away from the Fermi stage (Fig. 3) [28].

The diffusion length, L, is approximately related to the minority carrier lifetime τ_{bulk} by:

$$L = (D.\tau_{bulk})^{1/2} \qquad (1)$$

where D is the diffusion coefficient. In contrast to the electron-hole pairs' drift behaviour, the diffusion length, L, is independent of any built-in fields.

Both types of photo-generated carriers diffuse to the end surface in the same way, and their combination might cause data analysis mistakes, especially when the diffusion lengths exceed the wafer thickness. In actual semiconductors, the diffusion length is measured as:

$$L_{mean} = \sqrt{(D.\tau_{eff})} \qquad (2)$$

comprises the influence of surface recombination that is best known via its influence on carrier lifetime [27]:

$$1/\tau_{eff} = 1/\tau_{bulk} + 2.\frac{s}{d} \qquad (3)$$

where, τ_{eff} is the effective minority carrier lifetime, τ_{bulk} is the bulk minority carrier lifetime, s is the surface recombination velocity, and d is the wafer thickness.
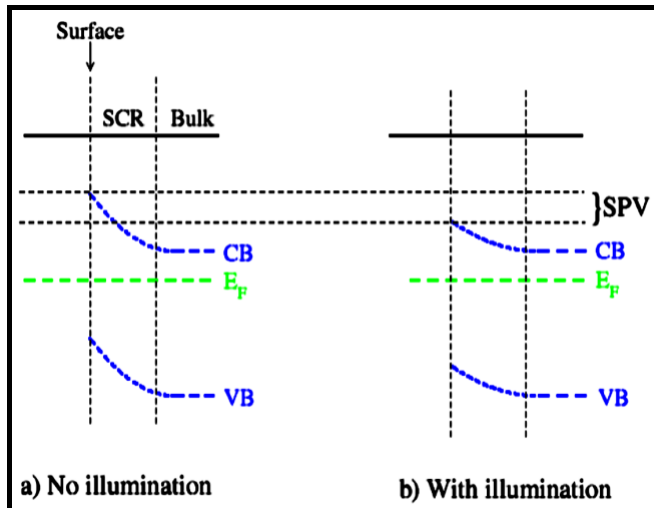
Fig. 3. Variation in surface potential: (a) no light illumination; (b) with light illumination.

3. Experimental set-up

This section provides a detailed description of light-induced surface photovoltage and efficiency measurements.

3.1 Surface photovoltage measurement

A basic, computer-controlled, normal incidence testing workbench was designed for light-induced surface photovoltage measurements of minority carrier lifetime of Si and other semiconductor wafers. The testing workbench is based on a stepper motor-driven small monochromator that can alter wavelengths in the 500-1200 nm spectral region. SPV is measured against the wavelength by means of a Stanford Research 510 lock-in amplifier. This method may be modified to quantify SPV against wavelength as well as flux density at a constant wavelength. For system control and data collecting, a LabVIEW system is used [17].

Figure 4 depicts comprehensive system diagrams of the minority carrier lifetime measurement system, in particular:
- 150W-fibre optical microscopic illuminator
- Stepper motor
- Motorized mini monochromator
- Aurum coated wafer chunk
- Light chopper
- Vacuum pump
- Contact probe
- Stanford research 510 lock-in amplifier
- Ito/Aurum coated quartz plate
- National Instruments USB 6008
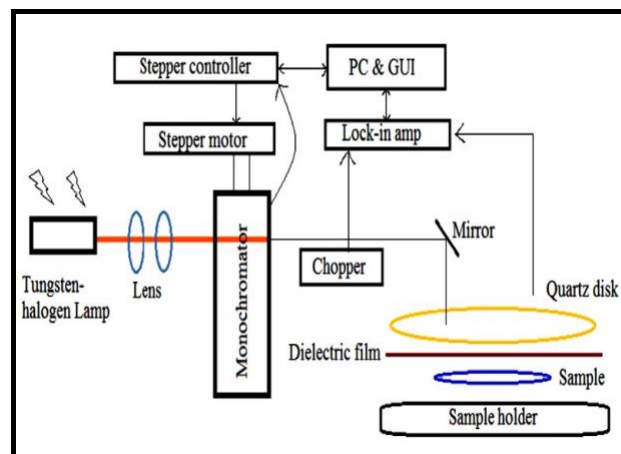
Fig. 4. Basic block diagram of the SPV measurement.

3.1.1. Mini monochromator

Motorised monochromator utilises a stepping motor driven by an external motor controller with RS 232 interface. Comprised with the controller is an application programme with above 25 instructions to control diverse manoeuvres of the grating drive. These motorised models also comprise a manual drive and a digital counter that shows the wavelength to 0.2 nm. Light from a tungsten-halogen lamp is concentrated on the entry slit of the monochromator (Fig. 5). The output from the monochromator is directed to the wafer vacuum chuck with a simple folding mirror. During normal operation, light from the outlet slit of the monochromator is directed to the wafer at normal incidence (Fig. 6).
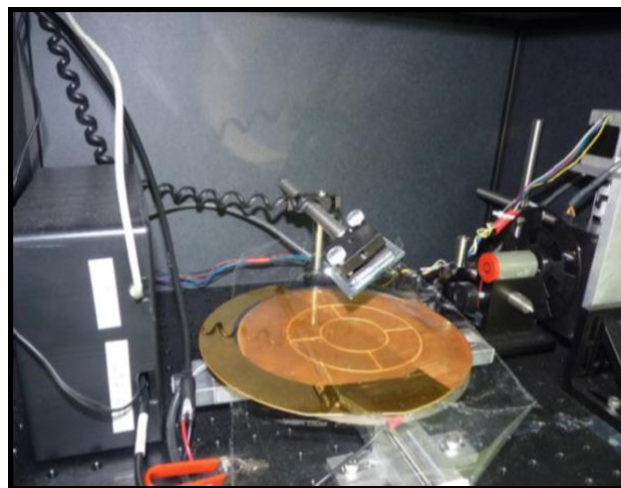
Fig. 5. Close-up views of the SPV system displaying wafer chuck, interface box, and the folding mirror.
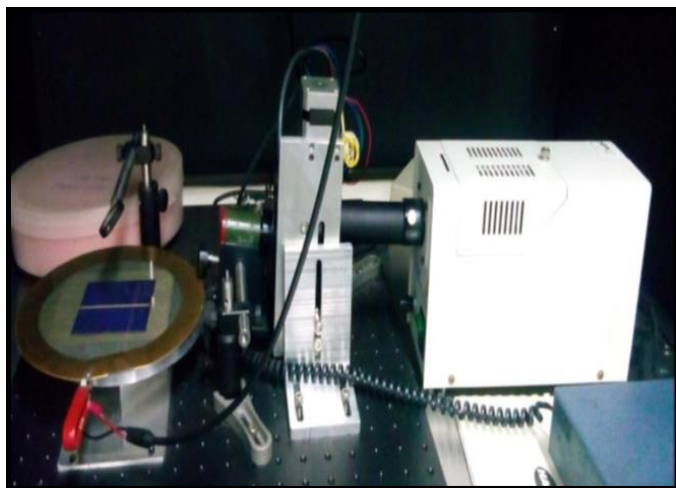
Fig. 6. 150W-fibre optical microscopic illuminator with motorised monochromator.

3.1.2. Stepper motor

To change the monochromator output wavelength, a stepper motor is used. Monochromator wavelength calibration is determined through electronic upper and lower limit switches. These limit switches are determined by moving the stepper motor to the limit switch. For example, the upper limit switch for this monochromator is set at 1205.7 nm and the lower at ~ 28 nm. Once the system finds the limit switch, wavelength is defined, and system is moved to desired wavelength by setting up known number of steps.

3.1.3. SR510 Lock-in amplifier

To detect and quantify very tiny ac signals, the Lock-in technique is used. Even when the signals are masked by noise sources a thousand times greater, a Lock-in amplifier can make precise measurements of minuscule signals. A PC with the LabVIEW platform controls the lock-in output and stepper motor. The wavelength range of the system is 500-1200 nm. Data is written to a text file for graphing and processing later.

To be in a relatively noiseless region of the noise spectrum, we chose a reference frequency of 5 kHz. Due to the RC time constant of the source impedance and the cable capacitance, this frequency is sufficiently high to prevent low frequency '1/f' noise, line noise, phase shifts, and amplitude errors.

The expected signal from our trial corresponds to the full-scale sensitivity of 100 nV. The sensitivity has been tuned to 1%. The measurement precision is also affected by the instrument's output stability. The output steadiness for the dynamic reserve in question is 0.1 percent /°C. A 1 percent inaccuracy is expected for a 10°C temperature difference.

3.1.4. Light chopper

The Model SR540 Optical Chopper is employed to square-wave modulate the intensity of optical signals. Light sources can be chopped at rates ranging from 4 Hz to 3.7 kHz. The synchronization signals required for a variety of operating modes are provided via adaptable, low jitter reference outputs: single or dual beam; sum and difference frequency; and synthesized chopping to 20 kHz.

3.1.5. ITO/Au coated quartz plate

Figure 7 shows how to detect capacitive SPV voltage by placing an ITO/Au coated quartz plate on top of the wafer to be tested. To create electrical isolation, a thin sheet of Teflon film is put between the top glass electrode and the wafer. The bottom electrode is Au-coated and connected to the Si wafer to reduce contact resistance. Figure 8 presents the SPV system with lock-in exhibiting signal of 0.74 V and frequency of 146 Hz.
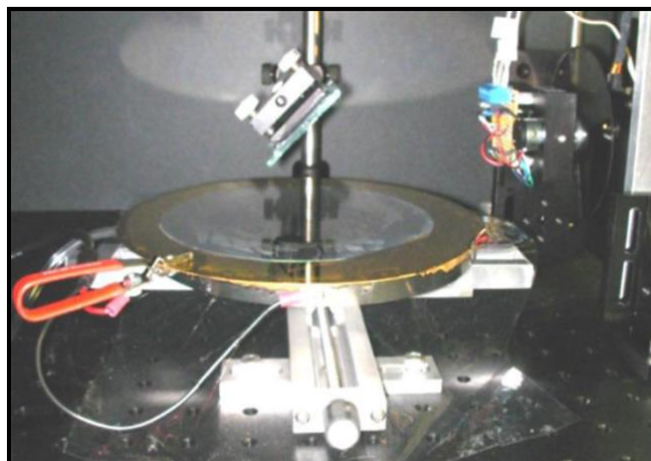
Fig. 7. The wafer under test inserted between the Au-coated chuck and ITO-coated quartz plate with Au-coated connections at edges.
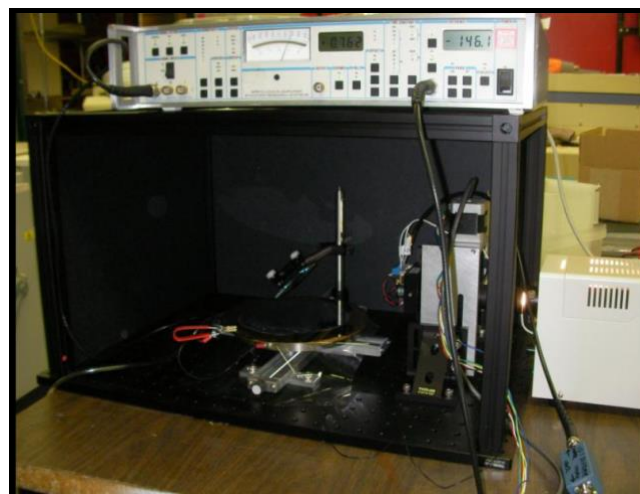
Fig. 8. SPV system with lock-in exhibiting signal of 0.74 V and frequency of 146 Hz.

3.1.6. Test setup procedure on computer data acquisition system

Prior to data acquisition, settings on the lock-in amplifier are manually set. This is done by looking at the SPV signal at wavelength of ~ 600 nm (red light). Following lock-in settings are fairly standard for these measurements:

- chopper frequency in ~ 30-200 HZ range,
- time constant ~ 100-300 ms,
- all input filters engaged,
- dynamic resolution off,
- offset off, and voltage scale is set anywhere between ~ 0.2 mV to 2 mV.

Once the lock-in settings are set, LabVIEW interface is used to acquire data by following the steps outlined below.

- Stepper motor speed is input; typically between 50–100 nm/min,
- Stepper motor is moved until upper limit switch corresponding to a wavelength of ~ 1205.7 nm is detected,
- Desired initial (λ_i) and final (λ_f) wavelengths are input for lifetime measurement scans,
- Incremental wavelength step (λ_s) in nm is input,
- At each wavelength position, SPV signal is acquired from the lock-in amplifier,
- Computer program calculates total number N of SPV measurements;
- $N = (\lambda_f - \lambda_i) / \lambda s$
- Computer moves stepper motor by increments of $(400/75).\lambda$ steps for each of the wavelength measurements,
- Computer program measures SPV at each wavelength $(\lambda_j) = \lambda_i + (\lambda_f - \lambda_i).j / N$, where N is the total number of measurements defined above, and j is each individual measurement,
- Once scan is completed, computer program writes the data file with two columns $(\lambda(j), V(j))$,
- After the file, if more scans are needed, procedure from steps i. through steps ix are repeated, and finally,
- If all data acquisition is completed, system requests that the wavelength be set at λ=600 nm so that alignment is visually convenient for next set of measurements.
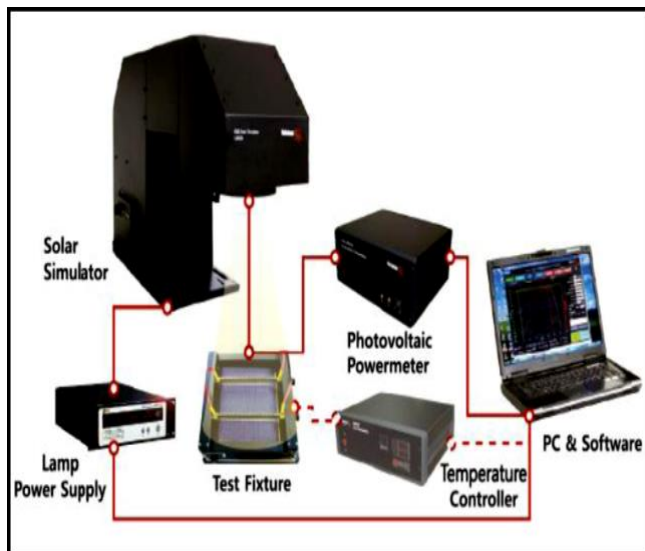
Fig. 9. Complete test setup of the system.

4. Experimental results and discussion

This section provides the test results along with a discussion of the minority carrier diffusion length and life duration, as well as efficiency.

4.1. Minority carrier diffusion length and life time

For conducting the experimental study, we have choose a reference cell from IIT, India of 156 cm² monocrystalline silicon solar cell.

LabVIEW results provide only the V_{SPV} in an arbitrary unit for the corresponding wavelength. To find the minority carrier diffusion length the penetration depth, α and reciprocal of penetration depth ($1/\alpha$) must be calculated. The penetration depth, α is related to the extinction coefficient, k using Equation (10) [30]:

Penetration Depth $\quad \alpha = \dfrac{4 . \pi . k}{\lambda} \quad$ (4)

where k is the extinction coefficient for Si. The term molar extinction coefficient (k) refers to the amount of light absorbed by a chemical species or substance at a specific wavelength. Λ is the wavelength of a light.

The data obtained from the SPV test and the penetration depth, α of the corresponding wavelength; reciprocal of penetration depth ($1/\alpha$) and the reciprocal of V_{SPV} are given in Table 1. The error bounds on the reported extinction coefficient data are expected to rise to $\pm$ 4% beyond 460 nm, and $\pm$ 10% beyond 1200 nm wavelength [17].

In SPV testing a computer-controlled monochromator illustrates the cell upon the test within a wide wavelength range (400-1200 nm). From the testing of SPV, the following graph is obtained as shown in Fig. 10. From the Table 1 and graphical representation of wavelength and V_{SPV} of Fig. 11, it can be concluded that from the wavelength of 780 nm to 840 nm we get the higher peak to compare to the other wavelength. Theoretically the available energy spectrum for silicon is in between 400 nm to 1100 nm and the range of higher peak value is 650 nm to 850 nm. If we compare this experimental result with the ideal one then it can be noticed that the result is almost comparable to the theoretical result of the solar spectrum of single junction silicon.
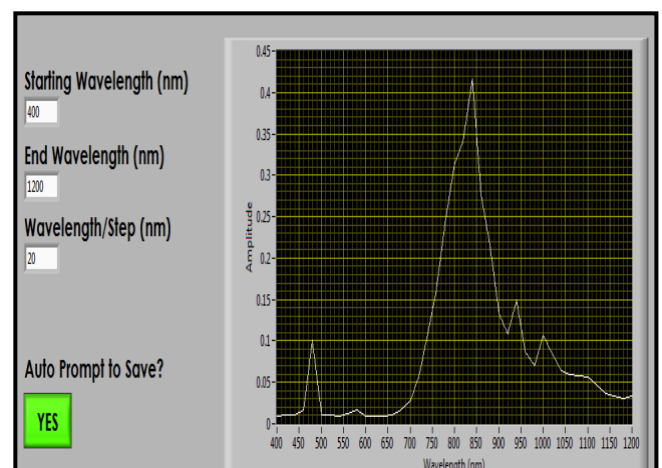
Fig. 10. Graphical representation of V_{SPV} vs wavelength from Labview.

Table 1. Data obtained from the SPV measurement system

Wavelength (nm)	V_{SPV} (arbitrary unit)	Extinction coefficient, k (Green and Keevers, 1995)	Penetration depth , α (cm^{-1}) (Green and Keevers, 1995)	Reciprocal of α (μm)	1/Vspv
400.0	0.009	0.303	9.52E+04	0.11	114.260
420.0	0.011	0.167	5.00E+04	0.20	89.047
440.0	0.010	0.109	3.11E+04	0.32	98.328
460.0	0.016	0.077	2.10E+04	0.48	61.091
480.0	0.100	0.057	1.48E+04	0.68	9.989
500.0	0.011	0.045	1.11E+04	0.90	87.658
520.0	0.011	0.036	8.80E+04	0.11	88.090
540.0	0.010	0.030	7.05E+03	1.42	101.071
560.0	0.012	0.026	5.78E+03	1.73	83.126
580.0	0.016	0.023	4.88E+03	2.05	60.617
600.0	0.009	0.020	4.14E+03	2.42	105.753
620.0	0.010	0.017	3.52E+03	2.84	103.199
640.0	0.010	0.015	3.04E+03	3.29	102.817
660.0	0.011	0.014	2.58E+03	3.88	92.098
680.0	0.016	0.012	2.21E+03	4.52	61.977
700.0	0.027	0.011	1.90E+03	5.26	37.376
720.0	0.057	0.010	1.66E+03	6.02	17.460
740.0	0.108	0.008	1.42E+03	7.04	9.235
760.0	0.151	0.007	1.19E+03	8.40	6.621
780.0	0.247	0.006	1.01E+03	9.90	4.051
800.0	0.312	0.005	8.50E+02	11.76	3.203
820.0	0.342	0.005	7.07E+02	14.14	2.925
840.0	0.417	0.004	5.91E+02	16.92	2.398
860.0	0.276	0.003	4.80E+02	20.83	3.621
880.0	0.217	0.003	3.83E+02	26.11	4.611
900.0	0.133	0.002	3.06E+02	32.68	7.533
920.0	0.108	0.002	2.40E+02	41.67	9.233
940.0	0.149	0.001	1.83E+02	54.64	6.706
960.0	0.087	0.001	1.34E+02	74.63	11.459
980.0	0.070	0.001	9.59E+01	104.28	14.319
1000.0	0.107	0.001	6.40E+01	156.25	9.367
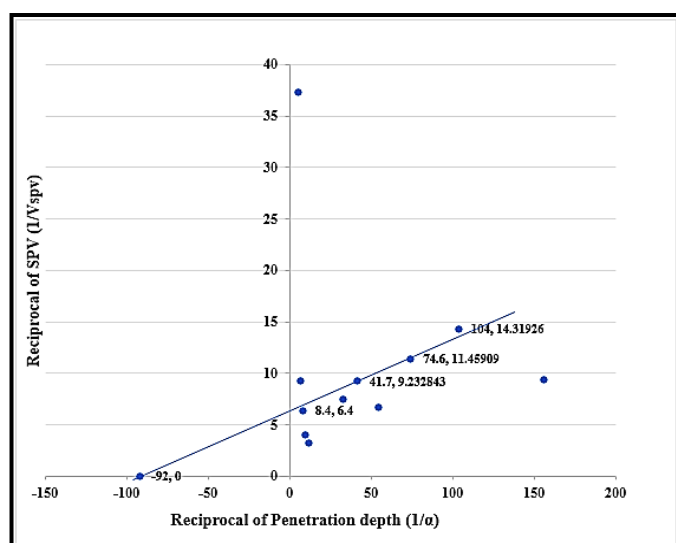
Fig. 11. Graphical representation of 1/V_{spv} Vs 1/α to define minority carrier diffusion length.

Minority carrier diffusion length can be calculated using SPV data. Three wavelengths of light can be used to do the measurement [32-34]. By adding more wavelengths and determining the best-fit straight line, an estimate can be made that is even more precise. Since the difference of penetration depth of 1/α between 700 nm and 780 nm is also slight rather than between 900 nm and 1000 nm, we use three distinct wavelengths (760 nm, 920 nm and 960 nm) to plot the best-fit straight line and determine minority career diffusion length and lifetime. The SPV data was graphed against reciprocal of penetration depth (1/α) and shown in Fig. 11. From the figure, the diffusion length can be estimated by its negative interception of the x-axis, which is 92 μm.

Therefore, the minority carrier lifetime is evaluated as follows:

$$\tau_n = \frac{L_n^2}{D} = 3.135 \ \mu s \qquad (5)$$

For crystalline silicon solar cells, the maximum carrier lifetime should be 1 millisecond, and the minority carrier

diffusion length should be in the region of 100-300 μm [35]. Therefore, our experimental test produces almost accurate results, i.e., a diffusion length of 92 μm. As stated, this value is in close proximity to the ideal value.

4.2. Efficiency measurement

The different areas from the same solar cell have been selected to measure the efficiency and analysis of the changes of data for different areas of a solar cell, and to verify the fabrication quality of a sample solar cell. From the examination of the simulation results on different areas, it can be concluded that the whole area of a solar cell is almost uniformly. From the sun simulator, the following results were obtained, which are presented in Table 2 below.

Table 2. Results from sun simulator

Parameter	Unit	Test Data		
		1	2	3
Area	cm^2	10.24	10.24	9
V_{OC}	V	0.609	0.611	0.599
I_{sc}	mA	595.678	598.187	604.619
J_{sc}	mA/cm^2	58.172	58.417	67.18
P_m	mW	164.381	164.878	148.995
V_m	V	0.357	0.365	0.337
I_m	mA	459.87	451.82	442.66
Fill Factor	%	45.35	45.09	41.11
Efficiency η	%	16.05	16.1	16.55
R_{SH}	Ω	20.542	14.338	6.184
R_S	Ω	0.495	0.494	0.542

The I-V curve (red graph) and P-V curve (green graph) have been plotted from test 1 data and depicted in Fig. 12. From Table 2, it can be stated that the efficiency for different areas is almost same. So it can be concluded that the cell is well fabricated and the efficiency is above 16%. Comparing the graphs from Figures 12 and 13 we can clearly state that our experimental data follow the ideal I-V characteristics of solar cell.
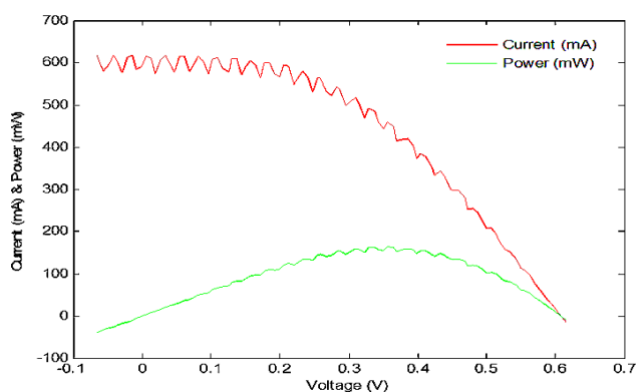
Fig. 12. I-V characteristics curve of sample solar cell.
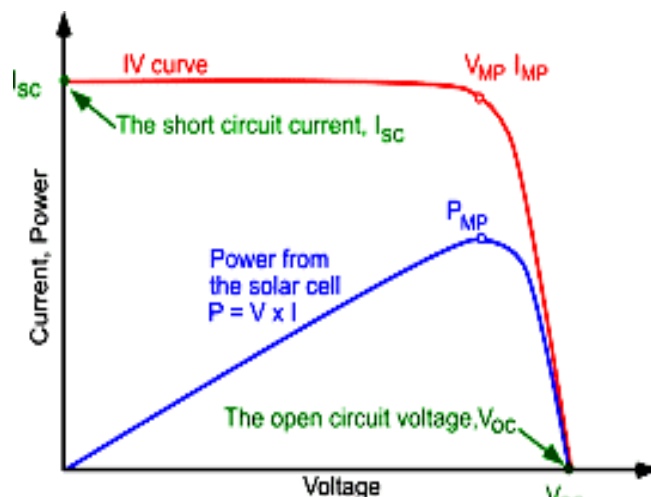
Fig. 13. Ideal I-V characteristics curve of solar cell [36].

5. Conclusions

This research paper offered two types of optical characterisation measurements, which were carried out successfully. The I-V characteristics of cells, as well as the minority carrier lifetimes, were investigated. SPV measurement instruments were provided by Institute of Electronics, Atomic Energy research Establishment, Savar, Dhaka, while the sun simulator was provided by Bangladesh Council of Scientific and Industrial Research (BCSIR). Results showed that the main advantage of SPV instrument is its comparatively low cost compared to other traditional methods.

The diffusion length of the minority carrier was frequently used to characterize the quality of silicon solar cell material before it was processed into solar cells, because it provides a prediction of the energy conversion efficiency that may be attained in the final form of the cells. The minority carrier lifetime is a very important parameter that aids the determination of the quality of a solar cell. The improved performance of the solar cells is a direct manifestation of reduction in the recombination of the surface of the charging carriers leading to an improvement in the current of the short circuits. This expectation is confirmed from the recombination life time measurements. It was observed that diffusion length sometimes created small values, which happened due to recombination method. It was also noticed that doping caused defects and more recombination. Again solar grade silicon wafer (purity six nines) also created some defects in the base region. So there must of necessity be a trade-off between excessive doping in order to increase the diffusion length and lifetime. The decrease of optical loss as well significantly supported to improve the minority carrier lifetime and other photovoltaic factors for instance *Im*, *Vm*, *J_{SC}*, *V_{OC}*, *FF*, and the solar cell efficiency. These results indicate that the loss in efficiency is clearly related to the high depth of the pores on the solar cell due to the enlarged surface recombination related to the augmented surface area.

By using sun simulator, the efficiency for different areas within the same solar cell was measured, which are 16.05, 16.10 and 16.55% and derived efficiency was found to

be above 16%. The drawbacks of this system, are maintenance difficulties, contact problems and high costs. The contact probes are the pin type that is useful for thin film solar cell. However due to the flexible mounting jig—measurement system it can also be used for monocrystalline Si-solar cell. In order for this to be possible, the cell was cut into 2cm/2cm size. Results appeared good when compared with another sun simulator operated by LIV software. In this model no attempt has been made to account for the effect of thickness in short-circuit current density equation which is principally responsible for the observed discrepancy. It has been concluded that this model would be useful for silicon solar cell performance parameter approximation if thickness is incorporated with short circuit current density equation.

Our future research will focus on optimising all of the obstacles and attempting to extend the length of diffusion in order to improve the efficiency of solar cells.

Acknowledgements

References

[1] J.S. Chiu, Y.M. Zhao, S. Zhang, D.S. Wuu, "The role of laser ablated backside contact pattern in efficiency improvement of mono crystalline silicon PERC solar cells", Solar Energy 196 (2020) 462–467.

[2] G. Li, Y. Lu, Q. Xuan, G. Pei, J. Ji, X. Zhao, "Performance analysis on a crystalline silicon photovoltaic cell under non-uniform illumination distribution with a high electrical efficiency", Solar Energy 203 (2020) 275–283.

[3] M.K. Basher, M.K. Hossain, M.A.R. Akand, "Effect of surface texturization on minority carrier lifetime and photovoltaic performance of monocrystalline silicon solar cell", Optik, 176 (2019) 93–101.

[4] H. Haug, C. Berthod, Å. Skomedal, J.O. Odden, E.S. Marstein, and R. Søndenå, "Simulated and measured temperature coefficients in compensated silicon wafers and solar cells", Solar Energy Materials and Solar Cells 200 (2019) 109921.

[5] X.Y. Chen, W.J. Xue, W.Z. Ban, X.L. Jiang, W. Shan, "Influence of the chemical composition in SiNx films on silver paste contact formation at silicon surface", Solar Energy 126 (2016) 105–110.

[6] A. Bougoffa, A. Zouari, E. Dhahri, "Analytical model of front texturization effect on silicon solar cell with porous silicon at the backside", Opt Quant Electron 49 (2017) 16.

[7] A. Castaldini, D. Cavalcoli, A. Cavallini, M. Rossi, "Surface photovoltage analysis of crystalline silicon for photovoltaic applications", Solar energy materials and solar cells, 72 (2002) 559–569.

[8] C. Marchat, J. P. Connolly, J. P. Kleider, J. Alvarez, L. J. Koduvelikulathu, J. B. Puel, "KPFM surface photovoltage measurement and numerical simulation", EPJ Photovoltaics, 10 (2019) 3.

[9] L. Kronik, Y. Shapira, "Surface photovoltage spectroscopy of semiconductor structures: at the crossroads of physics, chemistry and electrical engineering", Surf. Interface Anal. 31 (2001) 954–965.

[10] D. Cavalcoli, B. Fraboni, A. Cavallini, "Surface and Defect States in Semiconductors Investigated by Surface Photovoltage", Chapter 7, Semiconductors and Semimetals, Elsevier 91 (2015) 251–278.

[11] D. Cavalcoli, M. A. Fazio, "Electronic transitions in low dimensional semiconductor structures measured by surface photovoltage spectroscopy", Materials Science in Semiconductor Processing 92 (2019) 28–38.

[12] D. Bonkoungou, T. Guingane, E. Korsaga, S. Tassembedo, Z. Koalaga, F. Zougmore, A. Darga, "Measurements and analysis of the dark I-V-T characteristics of a photovoltaic cell: KX0B22-12X1F", Smart Grid (icSmartGrid) 2020 8th International Conference on, pp. 157–162, 2020.

[13] M.S. Esmaeili, G. Najafi. "Energy-Economic Optimization of Thin Layer Photovoltaic on Domes and Cylindrical Towers." International Journal of Smart Grid-ijSmartGrid 3 2 (2019) 84–91.

[14] M. J. Hossain, E. J. Schneller, M. Li, K. O. Davis, "Incorporation of spatially-resolved current density measurements with photoluminescence for advanced parameter imaging of solar cells", Solar Energy Materials and Solar Cells 199 (2019) 136–143.

[15] W. Kwapil, S. Wasmer, A. Fell, J. M. Greulich, M. C. Schubert, "Suns-ILIT: Contact-less determination of local solar cell current-voltage characteristics", Solar Energy Materials and Solar Cells 191 (2019) 71–77.

[16] D. Ma, W.J. Zhang, Z.Y. Jiang, Q. Ma, X.B. Ma, Z.Q. Fan, D.Y. Song, L. Zhang, "Microstructure and photoelectric properties of P-doped silicon-rich SiNx film as an n-type layer for PIN-type amorphous silicon thin film solar cells", Solar Energy 144 (2017) 808–817.

[17] M. A. Green, M. J. Keevers, "Optical properties of intrinsic silicon at 300 K", Progress in Photovoltaics: Research and applications 3 (1995) 189–192.

[18] A. Buczkowski, G. Rozganyi, F. Shimura, "Photoconductance minority carrier lifetime vs. surface photovoltage diffusion length in silicon", J. Electrochem. Soc. 140 (11) (1993) 3240.

[19] J. Lagowski, A.M. Kontkiewicz, L. Jastrzebski, P. Edelman, "Method for the measurement of long minority carrier diffusion lengths exceeding wafer thickness", P. Appl. Phys. Lett. 63 (21) (1993) 2902.

[20] A.L.P. Rotondaro, T.Q. Hurd, A. Kaniava, J. Vanhellemont, E. Simoen, M.M. Heyns, C. Claeys, "Impact of Fe and Cu contamination on the minority carrier lifetime of silicon substrates", J. Electrochem. Soc. 143 (1996) 3014–3019.

[21] M.S. Tyagi, R. Van Overstraeten, "Minority carrier recombination in heavily-doped silicon", Solid-State Electron. (1993) 577.

[22] A. Belkaid, I. Colak, K. Kayisli, M. Sara and R. Bayindir, "Modeling and Simulation of Polycrystalline Silicon Photovoltaic Cells," 2019 7th International Conference on Smart Grid (icSmartGrid), 2019, pp. 155–158, doi: 10.1109/icSmartGrid48354.2019.8990733.

[23] A. Parisi, L. Curcio, V. Rocca, S. Stivala, A. C. Cino, A. C. Busacca, G. Cipria, "Photovoltaic module characteristics from CIGS solar cell modelling", International Conference on Renewable Energy Research and Applications (ICRERA), 2013.

[24] G.M. Masters, Renewable and Efficient Electric Power Systems. John Wiley & Sons, 2004.

[25] Instruction Manual Flash LIV Solar Cell Tester, Institute of Electronics, Atomic Energy research Establishment, Savar, 2015.

[26] J. Toušek, D. Kindl, J. Touškova, Contactless photovoltage method for measurement of diffusion length of minority carriers in solar cells, Solar Energy Materials & Solar Cells 64 (2000) 29–35.

[27] A. Cuevas, D. Macdonald, Measuring and interpreting lifetime of silicon wafers, Solar Energy 76 (2004) 255–262.

[28] G. Hashmi, A.R. Akand, M. Hoq, "Study of the enhancement of the efficiency of the monocrystalline silicon solar cell by optimizing effective parameters using PC1D Simulation", Silicon 10 (2018) 1653–1660.

[29] R. Stangl, "Specific Characterization Method, Surface Photovoltage", Silicon Photovoltaic (2009) 1–3.

[30] D. K. Schroder, "Surface voltage & surface photovoltage: history, theory and applications", Meas. Sci. Technol. 12 (2001) 16–31.

[31] Dieter K Schroder, "Surface voltage & surface photovoltage: history, theory and applications", Meas. Sci. Technol. 12 (2001) 16–31.

[32] A.R. Akand, M. Rakibul Hasan, M. Khairul Basher, M. Hoq, "Study of Surface Photo voltage for monocrystalline silicon solar cell fabricated at BAEC solar cell lab", International Journal of Innovation and Applied Studies 7 (4) (2014) 1479–1484.

[33] R. O. Mahdi, J. E. Simon, O. N. Slman, "Measurement of diffusion length in P-N junction silicon solar cell". Al-Nahrain Journal of Science 11 (1) (2008) 59–63.

[34] M. R. Tur, İ. Colak, R. Bayindir, "Effect of Faults in Solar Panels on Production Rate and Efficiency," 2018 International Conference on Smart Grid (icSmartGrid), 2018, pp. 287-293, doi: 10.1109/ISGWCP.2018.8634509.

[35] N. Akter, Z. H. Mahmood, M. A. Tonima, M. Hoq, M. A. R. Akand, M. K. Basher, M. H. Ali, "Determination of Minority Carrier Diffusion Length by SPV Measurement for Calculation of Carrier Generation and Recombination of Silicon Solar Cell", ICMEIM, 2015.

[36] A. H. M. E. Reinders, P. J. Verlinden, W. G. J. H. M. van Sark, A. Freundlich, Photovoltaic Solar Energy: From Fundamentals to Applications. (Eds.), (2016), London, UK: Wiley & Sons. 665 p.